

Field trial of a 1.5 Tb/s adaptive and gridless OXC supporting elastic 1000-fold all-optical bandwidth granularity

N. Amaya,* G. S. Zervas, B. Rahimzadeh Rofoee, M. Irfan, Y. Qin, D. Simeonidou

School of Computer Science and Electronic Engineering, University of Essex, Colchester CO4 3SQ, UK
namaya@essex.ac.uk

Abstract: An adaptive gridless OXC is implemented using a 3D-MEMS optical backplane plus optical modules (sub-systems) that provide elastic spectrum and time switching functionality. The OXC adapts its architecture on demand to fulfill the switching requirements of incoming traffic. The system is implemented in a seven-node network linked by installed fiber and is shown to provide suitable architectures on demand for three scenarios with increasing traffic and switching complexity. In the most complex scenario, signals of mixed bit-rates and modulation formats are successfully switched with flexible per-channel allocation of spectrum, time and space, achieving over 1000-fold bandwidth granularity and 1.5 Tb/s throughput with good end-to-end performance.

©2011 Optical Society of America

OCIS codes: (060.4250) Networks; (060.4510) Optical communications.

References and links

1. O. A. Gerstel, "Flexible Use of Spectrum and Photonic Grooming," in *Photonics in Switching*, OSA Technical Digest (CD) (Optical Society of America, 2010), paper PMD3.
 2. P. J. Winzer, A. H. Gnauck, S. Chandrasekhar, S. Draving, J. Evangelista, and B. Zhu, "Generation and 1,200-km transmission of 448-Gb/s ETDM 56-Gbaud PDM 16-QAM using a single I/Q modulator," in 2010 36th European Conference and Exhibition on Optical Communication (ECOC), 19–23 Sept. 2010.
 3. S. Chandrasekhar and X. Liu, "Terabit superchannels for high spectral efficiency transmission," in 2010 36th European Conference and Exhibition on Optical Communication (ECOC), 19–23 Sept. 2010.
 4. J. Yu, Z. Dong and N. Chi, "Generation, Transmission and Coherent Detection of 11.2 Tb/s (112x100Gb/s) Single Source Optical OFDM Superchannel," in Optical Fiber Communication Conference (OFC 2011), 6–10 March 2011, paper PDP A6.
 5. B. Kozicki, H. Takara, Y. Tsukishima, T. Yoshimatsu, K. Yonenaga, and M. Jinno, "Experimental demonstration of spectrum-sliced elastic optical path network (SLICE)," *Opt. Express* **18**(21), 22105–22118 (2010).
 6. S. Thiagarajan, M. Frankel, and D. Boertjes, "Spectrum efficient super-channels in dynamic flexible grid networks - A blocking analysis," in 2010 36th European Conference and Exhibition on Optical Communication (ECOC), 19–23 Sept. 2010.
 7. O. Moriwaki, K. Noguchi, H. Takahashi, T. Sakamoto, K. I. Sato, H. Hasegawa, M. Okuno, and Y. Ohmori, "Terabit-scale compact hierarchical optical cross-connect system employing PLC devices and optical backplane," in National Fiber Optic Engineers Conference, OSA Technical Digest (CD) (Optical Society of America, 2010), paper PDPC9.
 8. H. Furukawa, T. Miyazawa, K. Fujikawa, N. Wada, and H. Harai, "First development of integrated optical packet and circuit switching node for new-generation networks," in 2010 36th European Conference and Exhibition on Optical Communication (ECOC), 19–23 Sept. 2010.
 9. D. Chiaroni, R. Urata, J. Gripp, J. E. Simsarian, G. Austin, S. Etienne, T. Segawa, Y. Pointurier, C. Simonneau, Y. Suzuki, T. Nakahara, M. Thottan, A. Adamiecki, D. Neilson, J. C. Antona, S. Bigo, R. Takahashi, and V. Radoaca, "Demonstration of the interconnection of two optical packet rings with a hybrid optoelectronic packet router," in 2010 36th European Conference and Exhibition on Optical Communication (ECOC), 19–23 Sept. 2010.
 10. H. Takara, B. Kozicki, Y. Sone, T. Tanaka, A. Watanabe, A. Hirano, K. Yonenaga, and M. Jinno, "Distance-adaptive super-wavelength routing in elastic optical path network (SLICE) with optical OFDM," in 2010 36th European Conference and Exhibition on Optical Communication (ECOC), 19–23 Sept. 2010.
 11. N. Amaya, G. S. Zervas, and D. Simeonidou, "Architecture on demand for transparent optical networks," *Transparent Optical Networks (ICTON), 2011 13th International Conference on*, 26–30 June 2011.
 12. "WaveShaper S-Series Product Brief," http://www.finisar.com/optical_instrumentation, October 2010.
 13. K. Nashimoto, D. Kudzuma, and H. Han, "High-speed switching and filtering using PLZT waveguide devices," in 2010 15th Optoelectronics and Communications Conference (OECC), 5–9 July 2010, pp. 540–542.
-

1. Introduction

There has been a considerable increase in the range of transmission rates and the spread between large and small bandwidth demands that current optical networks are required to provide [1]. Requirements for dissimilar data rates may arise from the geographic distribution of traffic or the variety of services provided. For instance, in some cases high-bit-rate traffic (e.g. 100 Gb/s) may be needed for datacenter interconnection, whilst other users may require transport of 100 Mb/s, 1 Gb/s and 10 Gb/s circuits. This vast range of traffic granularities is expected to expand in the future as networks migrate to support higher transmission rates beyond 100G. There is a significant amount of research focusing on high-capacity superchannels at 400 Gb/s [2], 1 Tb/s [3] and beyond [4]. Such superchannels may require channel spacings that would not be compatible with today's 100-GHz or 50-GHz ITU grid e.g. 75 GHz for 400 Gb/s and 150 GHz for 1 Tb/s. Hence, there has been growing interest in gridless and elastic optical networking [5,6] as a means to efficiently accommodate a mix of superchannels and low-speed channels as well as to improve point-to-point and overall network efficiency, e.g. 400G occupying 75-GHz bandwidth is more than twice as efficient as 100G using 50 GHz. On the other hand, efficient transport of lower bit-rate channels (e.g. hundreds of Mb/s) requires the implementation of sub-wavelength granularity whereby the transmission capacity of an optical channel is multiplexed among lower bit-rate demands. Thus, in the future optical network, optical nodes will need to allocate resources in a flexible and efficient manner to efficiently support high-speed channels (beyond 100G), lower speed channels (e.g. 40 Gb/s, 10Gb/s) and sub-wavelength channels (e.g. hundreds of Mb/s).

Meanwhile, a number of optical OXC architectures have been proposed to support various forms of optical switching such as MG-OXC [7], hybrid optical packet/circuit switch nodes [8], Packet-OADMs [9]. In addition, recent developments in elastic bandwidth allocation demonstrate the ability to deliver higher level of switching flexibility by the use of bandwidth adaptive (BA) wavelength selective switches (WSS) [10]. In this paper we are going beyond other efforts and demonstrate, for the first time, an adaptive optical cross-connect (OXC) that supports elastic allocation of arbitrary spectral, time and space resources per port in a symmetric or asymmetric manner. It can dynamically construct suitable architectures-on-demand tailored to traffic requirements. The system is implemented to transparently switch up to 1.5 Tb/s (160 Gb/s + 15x40 Gb/s + 74 x 10 Gb/s) of traffic with all-optical bandwidth granularities ranging from 143 Mb/s up to 160 Gb/s i.e. a factor of over 1000. Any OXC port is able to allocate any gridless spectrum-slice within the range of 12.5 GHz to 5 THz with a step size of 1 GHz, as well as perform elastic time-slice allocation varying from 1.06 μ s up to a maximum of continuous allocation in 1.06- μ s steps. The OXC is also able to optically groom individual channels or bands with different bit-rates (10Gb/s and 40Gb/s) as well as multicast continuous channels and sub- λ data flows.

2. Adaptive optical cross-connect

The adaptive optical cross-connect is based on the Architecture-on-Demand concept [11]. As illustrated in Fig. 1a, the system consists of an optical backplane, implemented using a 20ms 96x96 3D-MEMS optical switch, that inter-connects several architecture-building modules such as 200ms LCoS-based spectrum selective switch (SSS) [12], 10ns 2x2 PLZT optical switch [13], wavelength/waveband (De)-Multiplexer, 1x4 couplers and EDFAs. Modules are attached to the 3D-MEMS switch so that their inputs and outputs connect to the 3D-MEMS outputs and inputs respectively. Some of the MEMS ports are reserved as OXC inputs/outputs and add/drop according to the required node degree and add/drop capability. During operation, the switching requirements (spectrum-time-space) of the optical signals are used to compute a suitable arrangement and interconnection of the modules that delivers the required functionality. Such arrangement constitutes the required architecture of the OXC, which is implemented by means of internal cross-connections in the optical backplane. Figure 1a shows the cross-connections used in the optical backplane to construct the example architecture of Fig. 1b. As shown in Fig. 1b, individual arrangements of components, with

different levels of complexity, can be constructed on a per-port basis reflecting the switching requirements of the signals in each port. Such arrangements may be dynamically changed, by reconfiguring the backplane cross-connections, to fulfill the switching requirements of new traffic (Fig. 1c).

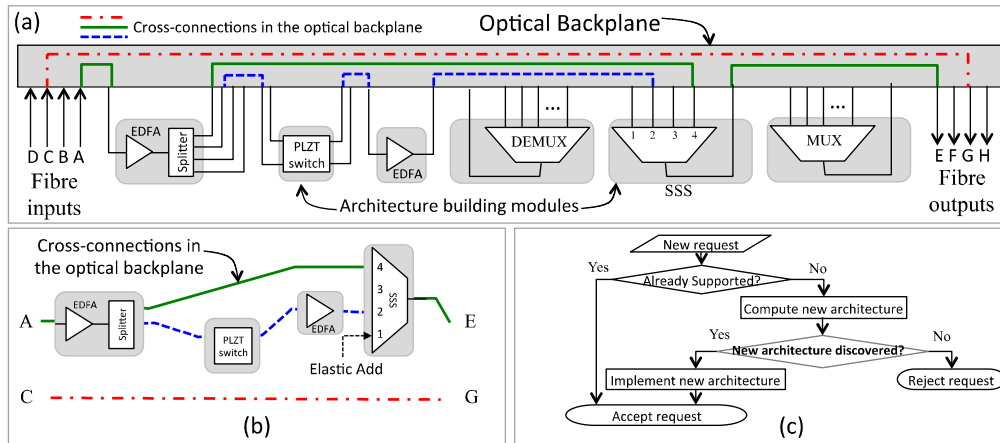


Fig. 1. a) Adaptive OXC, b) example architecture and c) architecture reconfiguration algorithm.

3. Field network and experimental setup

The network scenario, displayed in Fig. 2a, consists of three source nodes (A, B and C), one adaptive OXC (D) and three destination nodes (E, F and G). Nodes A and E are linked to D by dispersion compensated ITU-T G.652 installed fiber sections deployed in the UK between the University of Essex Labs in Colchester and Ipswich (80 km); and between the University of Essex Labs and Chelmsford (110 km), as shown in Fig. 2b. Channels are generated at the source nodes and transmitted to Node D where their switching requirements are used to construct a suitable architecture and switch the channels to their destination node(s).

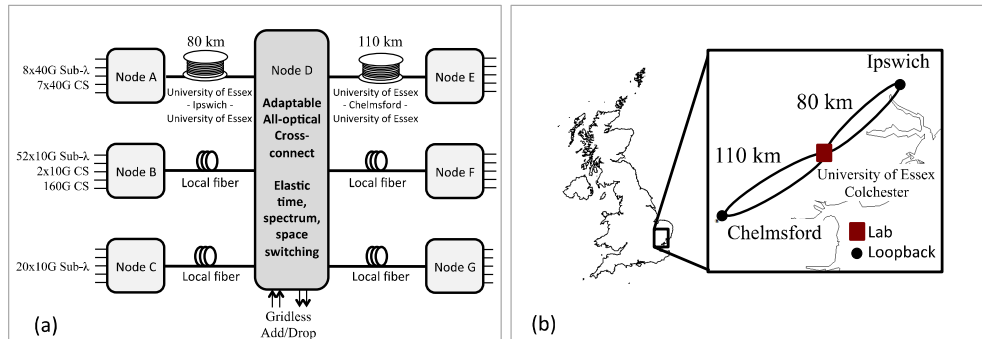


Fig. 2. a) Experimental network configuration and b) field fiber connectivity.

Figure 3 presents a more detailed representation of the experimental setup. At Node A, a multi-channel multi-format transmitter generates continuous 4x40 Gb/s NRZ and 3x40 Gb/s RZ plus 8x40 Gb/s RZ sub- λ channels, modulated with a PRBS7. Node B generates continuous 1x160 Gb/s RZ and 2x10 Gb/s NRZ data channels plus 52x10 Gb/s NRZ sub- λ data channels carrying PRBS7. Node C generates 20x10 Gb/s sub- λ channels with PRBS32 data. Flexible channel spacing is used depending on channel bandwidth and switching requirements; namely, 50 GHz for the 10 Gb/s, 100 GHz for the 40 Gb/s NRZ, 150 GHz for the continuous 40 Gb/s RZ and 200 GHz for the 40 Gb/s sub- λ channels. The 160 Gb/s RZ

signal requires a minimum spectrum allocation of 350 GHz. The OXC can support both 50/100 GHz ITU grid spacing as well as gridless / arbitrary spectrum spacing and allocation. The sub- λ channels are generated using fast tuneable lasers (<60 ns) according to a 68- μ s frame with variable time-slot size ranging from 1.06 μ s (147 Mb/s @ 10Gb/s and 590Mb/s @ 40 Gb/s) up to 67.94 μ s with 60-ns guard needed for C-Band λ tuning and switching.

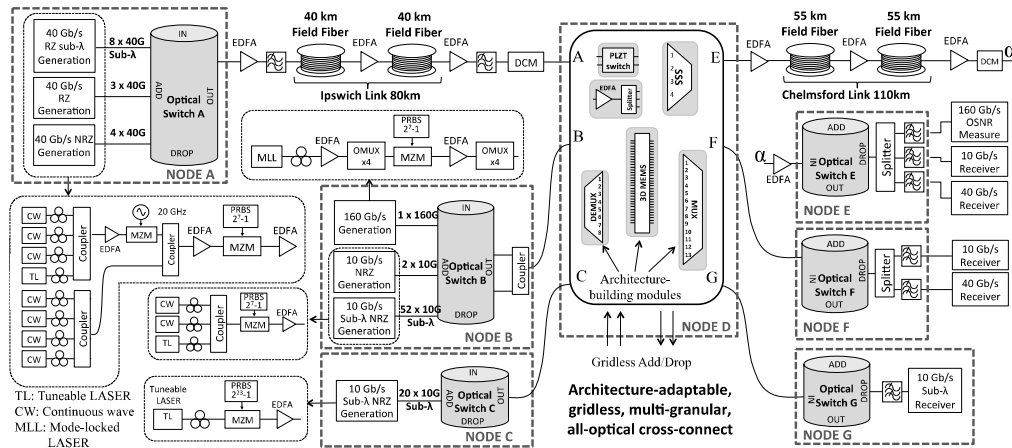


Fig. 3. Experimental Setup. Node D is the adaptive OXC.

3. Results and discussion

The flexibility of the proposed adaptive OXC is demonstrated in three scenarios with increasing traffic load and switching requirements. The on-demand architecture constructed in the first scenario demonstrates simultaneous wavelength and fiber switching on different ports of the adaptive OXC. For the second scenario a new architecture is dynamically constructed, which additionally implements waveband and arbitrary spectrum switching to fulfill the new switching requirements (e.g. 160Gb/s). Finally, the third architecture shows also multi bit-rate optical sub- λ grooming and multicasting. In addition, the 3rd scenario demonstrates flexible allocation of spectrum, space and time resources whereby the node transparently switches continuous and sub- λ channels and as such is able to time-multiplex arbitrary spectrum among sub- λ channels of different bit rates (10Gb/s and 40Gb/s) and modulation formats.

In the first scenario, Node A transmits 5x40 Gb/s sub-wavelength and 1x40 Gb/s NRZ continuous channel over the Ipswich link. As shown in Fig. 4a, Node E is the destination of these channels so they require to be switched to output E and transmitted over the Chelmsford link. Node B generates 8x10 Gb/s sub-wavelength channels that go towards either Node E (three channels) or Node F (five channels). Node C generates 20x10 Gb/s sub-wavelength channels, all with destination Node G. The architecture required to provide this switching functionality, shown in Fig. 4a, is implemented by establishing the required cross-connections in the optical backplane. It consists of one wavelength de-multiplexer to split the signals from Node B, one multiplexer to re-combine the signals going towards Node F, one amplifier and two couplers to merge the signals going towards Node E. Node C traffic is switched using a single 3D-MEMS cross-connection to Node G.

In the second scenario, displayed in Fig. 4b, Nodes A and B have additional traffic and switching requirements. Node A transmits 4x40 Gb/s continuous NRZ and 10x40 Gb/s sub- λ RZ signals over the Ipswich link, some of which go to Node E and some to Node F. Node B generates 54x10 Gb/s NRZ and one 160 Gb/s signal. The 160 Gb/s signal requires to be switched towards Node E together with 39x10 Gb/s channels, the 18x10 Gb/s channels remaining go to Node F. The required architecture is implemented by reconfiguring the cross-connections in the 3D-MEMS switch, as shown in Fig. 4b. A 1x4 200-ms LCoS-based SSS that supports flexible spectrum allocation per port (multiple bands of variable size from 12.5-

GHz up to 5-THz bandwidth in 1-GHz steps) is used to switch the 160 Gb/s signal by programming a co-centered 600-GHz band to be passed from port 1 to its common port. Also, for the 10 Gb/s and 40 Gb/s signals destined towards Node E customized bandwidths per channel are used according to individual channel bandwidths. For the signals going to Node F, 150-GHz (De)-Multiplexer are used to switch either a single 40 Gb/s channel or three 10 Gb/s channels per MUX/DEMUX port as in waveband switching [7].

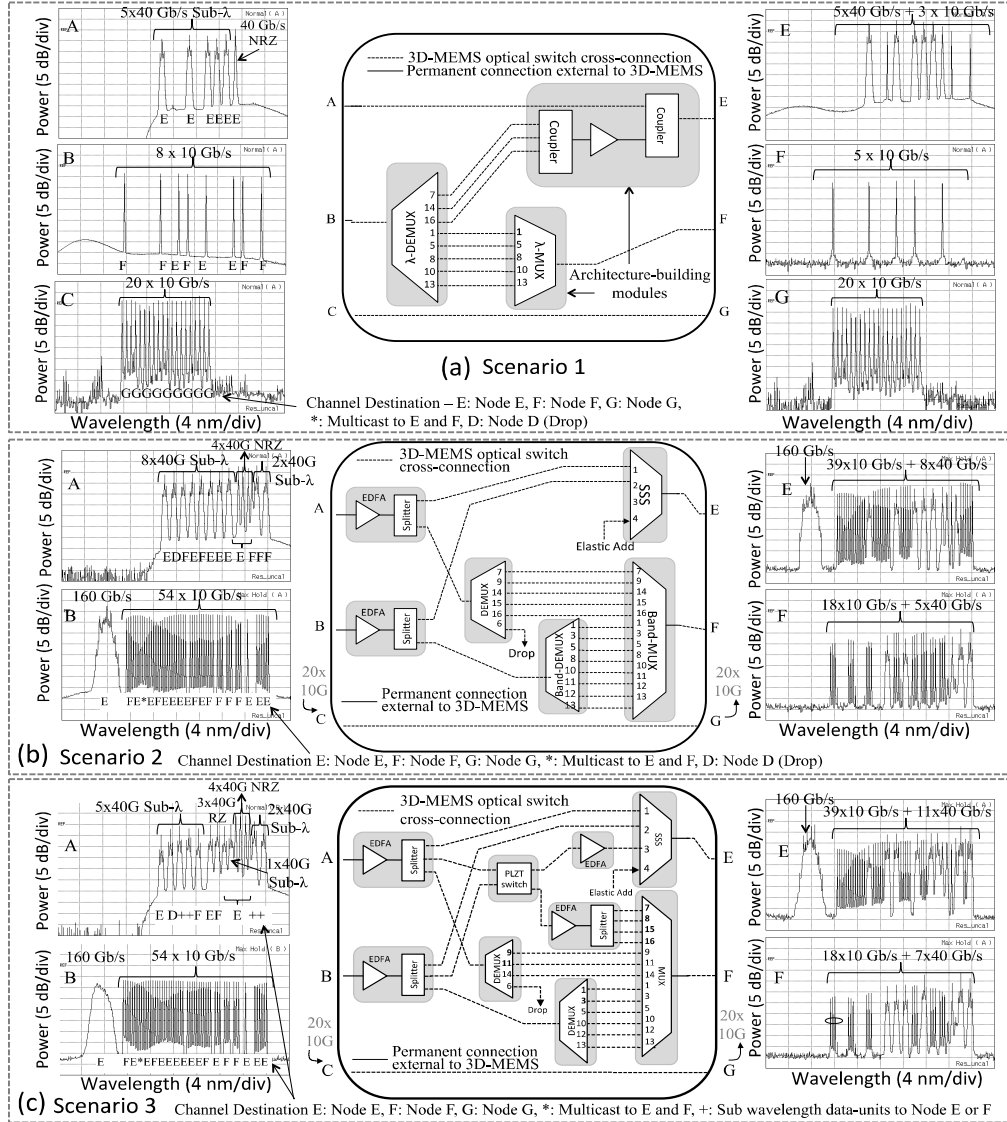


Fig. 4. Constructed architectures and spectrum plot results for three traffic scenarios.

In the third scenario, Fig. 4c, Node A traffic is increased by three continuous 40 Gb/s RZ and one sub- λ 40 Gb/s RZ channel. In order to free up spectrum for the new channels, three sub- λ 40 Gb/s channels are tuned to share the same λ with other sub- λ channels, i.e. multiplexed in time. Therefore, data-units from Node A transmitted at the same λ but at different time intervals may have different destinations, as shown in Fig. 5b, and need to be switched independently. This new requirement of sub- λ and sub-band switching is not accomplished by the architecture of the previous scenario. Therefore, a new configuration

(Fig. 4c) is implemented by re-configuring the 3D-MEMS switch. Thus, sub- λ data-units coming from Node A are switched to the appropriate destination using a 10-ns PLZT switch.

Data-units that go towards Node E are groomed with one 3x10-Gb/s sub-band channel, which goes to the same destination and uses the same spectrum, selected on port 3 of the SSS and transmitted over the Chelmsford link. Data-units that go towards Node F are output on port 4 of the PLZT switch, amplified and replicated. Then, copies are input to the ports of the multiplexer that correspond to the λ s of the data-units. Figure 5a shows an example 68- μ s frame of a 10 Gb/s sub- λ channel with allocated flexible data-unit sizes of 1.06 μ s, 4.2 μ s and 17 μ s. The minimum data-rate unit switched with this architecture is a 10 Gb/s sub- λ channel occupying one 1.06- μ s slot in the 68- μ s frame (\sim 147 Mb/s) and the maximum is the 160 Gb/s RZ continuous channel. Hence, the bandwidth granularity factor is greater than 1000. In scenarios 2 and 3, three 10-Gb/s channels are multicast to Nodes E and F. Also, in all three scenarios, architectures are built using multiple switching stages (1&2 stages for scenarios 1 and 2, and 1,2&3 stages for scenario 3). EDFAs are used to compensate for the insertion loss of internal node paths and balance the power of all channels on each output port with less than 1.5-dB deviation. Figure 5b shows the 10&40 Gb/s sub- λ data-units switched from A and B to E and F together with their eye diagrams. The average penalty of the node was 1 dB with a maximum of 2 dB for 40G sub- λ due to additional loss in PLZT switch. The average end-to-end network penalty was 2.5 dB and the maximum 4.5 dB was measured for the 40 Gb/s NRZ continuous channels. For the 160 Gb/s channel we measured a back-to-back Q-factor of 19.1 dB and an end-to-end degradation of 2.1 dB. The 40G sub- λ channels showed an enhanced sensitivity compared to continuous channels due to the higher ratio of peak to average power.

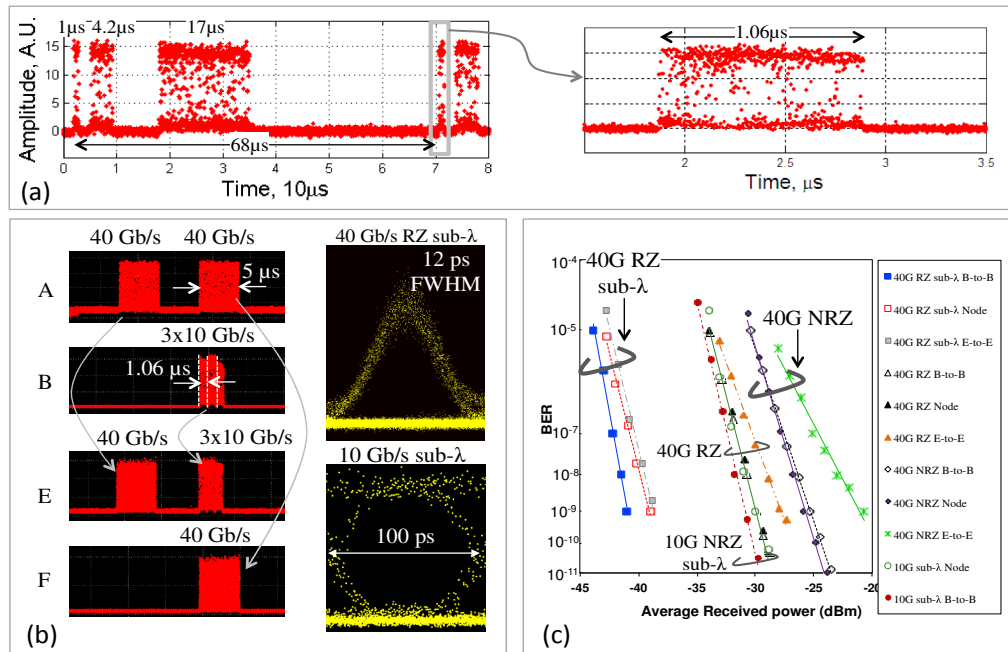


Fig. 5. a) Example frame showing flexible time allocation, b) time multiplexing of 40 Gb/s and 3x10 Gb/s and c) BER results for 10 Gb/s and 40 Gb/s continuous and sub- λ channels in Scenario 3.

4. Conclusion

We have presented an adaptive OXC that dynamically constructs architectures tailored to traffic requirements and supports elastic allocation of arbitrary spectral and time resources. The system is evaluated in a network of seven nodes and installed fiber with three different

traffic scenarios. It is shown to switch up to 1.5 Tb/s based on continuous and sub- λ signals at 160 Gb/s, 40 Gb/s and 10 Gb/s, with over 1000-fold all-optical bandwidth granularity factor.

Acknowledgements

This work is supported by the EC FP7, grant agreement No. 247674, STRONGEST and the EPSRC grant EP/I01196X: Transforming the Future Internet: The Photonics Hyperhighway. The authors acknowledge EpiPhotonics for the fast switch loan.